First-principles study of equilibrium properties and electronic structure of $Ti_3Si_{0.75}Al_{0.25}C_2$ solid solution

2003 J. Phys.: Condens. Matter 15 5959

(http://iopscience.iop.org/0953-8984/15/35/305)

INSTITUTE OF PHYSICS PUBLISHING JOURNAL OF PHYSICS: CONDENSED MATTER

J. Phys.: Condens. Matter **15** (2003) 5959–5968 PII: S0953-8984(03)63266-2

First-principles study of equilibrium properties and electronic structure of $Ti_3Si_{0.75}Al_{0.25}C_2$ solid solution

J Y Wang[1,2] **and Y C Zhou**[1]

[1] Shenyang National Laboratory for Materials Science, Institute of Metal Research, Chinese Academy of Sciences, Shenyang 110016, People's Republic of China
[2] International Centre for Materials Physics, Institute of Metal Research, Chinese Academy of Sciences, Shenyang 110016, People's Republic of China

Received 8 May 2003, in final form 27 June 2003
Published 22 August 2003
Online at stacks.iop.org/JPhysCM/15/5959

Abstract

Based on first-principles pseudopotential total energy calculations, the effects of Al substitution in Ti_3SiC_2, yielding chemical formula $Ti_3Si_{0.75}Al_{0.25}C_2$, were studied by examining the equilibrium properties and electronic structure. The lattice configurations, cohesive energy, atomic bonding properties and bulk modulus, as well as the electronic band structure, were investigated. Firstly, we obtained the equilibrium crystal parameters that included lattice constants, internal atomic coordinates and bond lengths. Then, the degrees of Ti–Si, Ti–C and Ti–Al covalent bondings in $Ti_3Si_{0.75}Al_{0.25}C_2$ were illustrated and compared with the corresponding values in Ti_3SiC_2 and Ti_3AlC_2 compounds. Furthermore, the magnitude and anisotropy of electrical conductivity were discussed by investigating the density of states and band structure. The bulk modulus of $Ti_3Si_{0.75}Al_{0.25}C_2$ yielded a value close to that of Ti_3AlC_2, which indicated the high bulk modulus had been preserved. In addition, we predicted better oxidation resistance of $Ti_3Si_{0.75}Al_{0.25}C_2$ than that of Ti_3SiC_2, and this was recently verified by an isothermal oxidation experiment of Al-cemented Ti_3SiC_2-based ceramic.

1. Introduction

The layered ternary ceramics with the common formula of $T_{n+1}AX_n (n = 1–3)$, where T is a transition metal, A is a group IIIA or IVA element and X is carbon or nitrogen, combine excellent properties of metals and ceramics. The astonishing properties include high melting point, low density, good thermal and electrical conductivity, high bulk modulus, excellent thermal shock resistance and high temperature oxidation resistance, damage tolerance and microscale ductility at room temperature etc [1]. Among the family of layered ternary compounds, titanium silicon (or aluminium) carbides, such as Ti_3SiC_2, Ti_3AlC_2 and Ti_2AlC, promoted comprehensive research activities because of their explicit industrial application prospects. Up to the present, these carbides have been demonstrated to be promising candidates

for high temperature structural applications, owing to the features of low density, good oxidation resistance and high temperature strength.

As a critical property at high temperature, the abilities to resist oxidation for Ti_3SiC_2 and Ti_3AlC_2 were widely investigated in recent years [2–4]. Despite the different methods for synthesizing bulk materials, some widely accepted conclusions were stated. For example, the parabolic oxidation behaviour was reported by Sun *et al* [2] and Barsoum and El-Raghy [3] for Ti_3SiC_2 and Wang and Zhou for Ti_3AlC_2 [4]. The parabolic rate constant of Ti_3SiC_2 yielded 4×10^{-7} kg^2 m^{-4} s^{-1} at 1100 °C [2], while the corresponding value of Ti_3AlC_2 was 2.7×10^{-10} kg^2 m^{-4} s^{-1} [4], which was about three orders smaller in magnitude. This indicated that the Ti_3AlC_2 compound possessed better ability to resist oxidation than Ti_3SiC_2 at high temperatures.

Ti_3SiC_2 and Ti_3AlC_2 were isotypic compounds, in which two edge-shared layers of Ti_6C octahedral groups were linked by two-dimensional closed-packed Si or Al atomic layers. It was known that good oxidation resistance attributed to the formation of protective scale, such as SiO_2 for Ti_3SiC_2 and α-Al_2O_3 for Ti_3AlC_2, on the subsurface at high temperatures. In addition, the diversity of oxidation behaviour between Ti_3SiC_2 and Ti_3AlC_2 was expected to mainly derive from the difference on Ti–Si and Ti–Al interlayer interactions. Although Ti_3SiC_2 displayed many unique properties, its unsatisfied oxidation resistance frustrated technological applications. An important task was to optimize the property of oxidation resisting for Ti_3SiC_2 with proper methods, such as alloying or solid solution treatment. According to previous investigations, a natural thought was to synthesize the Ti_3SiC_2-based solid solution with Al substitution.

Compared to the comprehensive knowledge on the properties of stoichiometric layered ternary ceramics, less information was available for the solid solution counterparts. Nowotny and collaborators [5] investigated the crystal chemistry of some complex H-phase carbides and related compounds. Recently, Barsoum and co-workers studied the mechanical, thermal and electrical properties of $(Ti, Nb)_2AlC$ [6] and $Ti_2Al(CN)$ [7] solid solutions in experiments. The only theoretical research was concentrated on the electronic structure of Ti_3SiCN and Ti_3SiCO [8], but the results were not associated with other properties there. As far as we are aware, no investigations on properties of Ti_3SiC_2-based solid solution with Al substitution have been reported until now.

First-principles electronic structure calculations have demonstrated usefulness in studying the important materials characteristics of Ti_3SiC_2 [9, 10] and Ti_3AlC_2 [11]. For example, the equilibrium geometrical parameters were well reproduced [9, 11], and the mechanism of mechanical stability under high pressure was exhibited [10]. In the present work, we were inspired to answer two questions: one was the effect of Al substitution on equilibrium properties and electronic band structure, and the other was the possibility to optimize the behaviour of oxidation resistance of Ti_3SiC_2 by such treatment. Here, we substituted a small amount of Si with Al atoms to build up the Ti_3SiC_2-based solid solution. As a first step, the present paper dealt with one chemical formula, $Ti_3Si_{0.75}Al_{0.25}C_2$, only.

2. Crystal structure aspects and method of calculation

The equilibrium crystal structures of Ti_3SiC_2 and Ti_3AlC_2 were investigated both by experiments [12, 13] and first-principles calculations [11, 14]. For Ti_3SiC_2, the lattice constants observed in experiment [12] were $a = 3.067$ Å and $c = 17.671$ Å, while the theoretical values [14] were $a = 3.071$ Å and $c = 17.670$ Å, respectively. For Ti_3AlC_2, the lattice constants yielded $a = 3.075$ Å and $c = 18.578$ Å in experiment [13], and $a = 3.072$ Å and $c = 18.732$ Å in *ab initio* calculation [11]. The *ab initio* values agreed with experimental

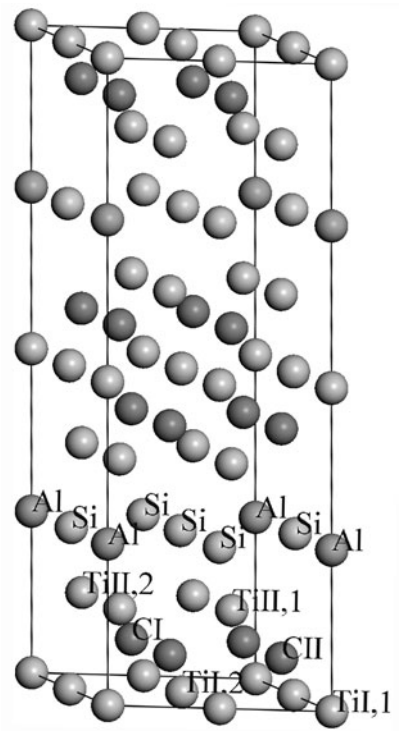

Figure 1. Crystal structure of supercell with chemical formula $Ti_3Si_{0.75}Al_{0.25}C_2$.

results well. They showed reliable ability in predicting the equilibrium properties of this class of layered ternary compounds by quantum mechanics scale calculations.

In order to compare the equilibrium crystal structure and electronic band structure, we performed total energy calculations for the three compounds, Ti_3SiC_2, Ti_3AlC_2 and $Ti_3Si_{0.75}Al_{0.25}C_2$, with respect to full geometry optimizations. The crystal structures of Ti_3SiC_2 and Ti_3AlC_2 unit cell were similar to that illustrated before [14], in which the unit cell contained 12 atoms. The crystal structure of $Ti_3Si_{0.75}Al_{0.25}C_2$ solid solution was represented by a 48-atom supercell, for which the unit cell of Ti_3SiC_2 was doubled both in *a* and *b* directions and a certain number of Al atoms substituted in the place of Si atoms, as shown in figure 1. In previous investigations Ti atoms were typically indexed with Ti_I and Ti_{II} owing to the structurally non-equivalent positions, while in the present work the Ti atoms were indexed with four notations, $Ti_{I,1}$, $Ti_{I,2}$, $Ti_{II,1}$ and $Ti_{II,2}$, corresponding to different coordinating environments with C, Si and Al atoms. For consistency, the C atoms were subdivided into C_I and C_{II}, respectively.

The equilibrium crystal parameters and ground-state electronic band structure were calculated by using the CASTEP code, in which a plane-wave pseudopotential total energy calculation was performed based on density functional theory [15]. The plane-wave basis set cut-off is selected as 450 eV, which was sufficient in leading to good convergence for total energy and forces acting on the atoms. The interactions of the electrons with the ion cores were represented by Vanderbilt-type ultrosoft pseudopotentials for Ti, Si, Al and C atoms [16]. The electronic exchange–correlation energy was treated under the local-density approximation scheme [17]. A Monkhorst–Pack mesh [18] of $8 \times 8 \times 2$ special $\boldsymbol{k}$-points sampling was chosen in all total energy calculations. Details of calculation of the partial density of states can be referred to in [10].

Table 1. Calculated lattice parameters, cohesive energy E_{coh}, bulk modulus B_0 and density of states at the Fermi level $N(E_F)$ of $Ti_3Si_{0.75}Al_{0.25}C_2$, Ti_3SiC_2 and Ti_3AlC_2.

Compound	Lattice parameters			E_{coh} (eV/atom)	B_0 (GPa)	$N(E_F)$ (states/eV/u.c.)
	a (Å)	c (Å)	c/a			
Ti_3SiC_2	3.0563	17.6604	5.7784	8.07	197	5.04
$Ti_3Si_{0.75}Al_{0.25}C_2$	3.0624	17.7050	5.7813	7.98	188	4.09
Ti_3AlC_2	3.0634	18.5066	6.0412	7.70	187	3.76

Table 2. Atomic internal coordinates of $Ti_3Si_{0.75}Al_{0.25}C_2$, Ti_3SiC_2 and Ti_3AlC_2.

Atoms	Atomic fractional positions		
	$Ti_3Si_{0.75}Al_{0.25}C_2$	Ti_3SiC_2	Ti_3AlC_2
$Ti_{I,1}$	0, 0, 0	0, 0, 0	0, 0, 0
$Ti_{I,2}$	0.5, 0.5, 0		
$Ti_{II,1}$	0.6667, 0.3333, 0.1655	0.6667, 0.3333, 0.1366	0.6667, 0.3333, 0.1286
$Ti_{II,2}$	0.6644, 0.3322, 0.1341		
Si	0.4956, 0.5044, 0.25	0.5, 0.5, 0.25	
Al	0, 0, 0.25		0, 0, 0.25
C_I	0.6667, 0.3333, 0.5717	0.6667, 0.3333, 0.5728	0.6667, 0.3333, 0.5699
C_{II}	0.6658, 0.8329, 0.5725		

3. Results and discussion

3.1. Equilibrium and cohesive properties

To investigate the ground-state properties of Ti_3SiC_2, Ti_3AlC_2 and $Ti_3Si_{0.75}Al_{0.25}C_2$, we obtained the structural configurations that possessed the local minimum total energy at first. In table 1, the optimized lattice constants for the three compounds are listed and compared. The *ab initio* lattice parameters of Ti_3SiC_2 and Ti_3AlC_2 agree with experimental values [12, 13] well. This ensures the reliability of the calculated lattice parameters of $Ti_3Si_{0.75}Al_{0.25}C_2$. The equilibrium lattice constants of $Ti_3Si_{0.75}Al_{0.25}C_2$ exhibit an interesting reminiscence of those of Ti_3SiC_2 and Ti_3AlC_2, respectively. a along the basal plane expands to a value very close to that of Ti_3AlC_2, while c remains similar in value to that of Ti_3SiC_2. The results imply that atomic bonds are disturbed by substituting a small amount of Si with Al atoms.

The internal atomic positions of the three compounds are exhibited in table 2, respectively. It is found that the internal freedoms change in different levels because of various coordinating configurations. The Ti_{II} atoms are no longer located in the same (001)-like close-packed atomic plane, as well as the C atoms. This is associated with the distortion of the Ti_6C octahedron, which is derived from the changes of bonding properties. Although we focus on the crystal structure of Ti_3SiC_2-based solid solution with only one chemical composition, the obtained data can be used to identify the $Ti_3(Si_{1-x}Al_x)C_2$ phase in experimental observations. For example, the structural parameters can be used to simulate the ideal x-ray diffraction pattern, in which one can easily trace the tendency of changes in relative intensities and positions of corresponding characteristic diffraction peaks.

The cohesive energy was a measure of the strength of the forces that bind atoms together in the solid state and was very descriptive in studying the phase equilibrium. The cohesive energy $E_{coh}^{Ti_3Si_{0.75}Al_{0.25}C_2}$ of $Ti_3Si_{0.75}Al_{0.25}C_2$ solid solution was defined as the total energy of the

constituent atoms at infinite separation minus the total energy of the compound,

$$E_{\mathrm{coh}}^{Ti_3Si_{0.75}Al_{0.25}C_2} = [3E_{\mathrm{atom}}^{\mathrm{Ti}} + 0.75E_{\mathrm{atom}}^{\mathrm{Si}} + 0.25E_{\mathrm{atom}}^{\mathrm{Al}} + 2E_{\mathrm{atom}}^{\mathrm{C}}] - E_{\mathrm{total}}^{Ti_3Si_{0.75}Al_{0.25}C_2} \quad (1)$$

where $E_{\mathrm{total}}^{Ti_3Si_{0.75}Al_{0.25}C_2}$ referred to the total energy of $Ti_3Si_{0.75}Al_{0.25}C_2$ at equilibrium configuration and $E_{\mathrm{atom}}^{\mathrm{Ti}}$, $E_{\mathrm{atom}}^{\mathrm{Si}}$, $E_{\mathrm{atom}}^{\mathrm{Al}}$ and $E_{\mathrm{atom}}^{\mathrm{C}}$ were the pseudo-atomic energies of the pure constituents. The pseudo-atomic energies were calculated in the same CASTEP code by using the plane-wave basis. The box sizes for energy calculations were the same as the dimension of the supercell, in which the pseudo-atoms were located at the box centre, respectively. The cohesive energies of stoichiometric Ti_3SiC_2 and Ti_3AlC_2 were also calculated according to equation (1) for the sake of comparison. The calculated cohesive energies yield 8.07 eV/atom for Ti_3SiC_2, 7.98 eV/atom for $Ti_3Si_{0.75}Al_{0.25}C_2$ and 7.70 eV/atom for Ti_3AlC_2, as shown in table 1 respectively. It is noted that the cohesive energies of the three compounds are very close in magnitude, and the value of $Ti_3Si_{0.75}Al_{0.25}C_2$ locates between that of Ti_3SiC_2 and Ti_3AlC_2. This obviously indicates that the $Ti_3Si_{0.75}Al_{0.25}C_2$ phase is less stable than Ti_3SiC_2, but more stable than Ti_3AlC_2. It also demonstrates that it is possible for $Ti_3Si_{0.75}Al_{0.25}C_2$ to co-exist with the other two compounds from the viewpoint of energy favourability.

Sequentially, we examined the total energy as a function of the volume of the $Ti_3Si_{0.75}Al_{0.25}C_2$ supercell, as well as for Ti_3SiC_2 and Ti_3AlC_2. At each specified volume, c/a was fixed at the equilibrium value for each compound, and the internal atomic coordinates were well optimized. The energy–volume curves $E(V)$ for the three compounds were fitted by a third-order polynomial, and the bulk modulus B_0 was obtained as follows:

$$B_0 = V_0 \left.\frac{\partial^2 E(V)}{\partial V^2}\right|_{V_0} \quad (2)$$

where V_0 was the equilibrium volume.

The bulk modulus yields 188 GPa for $Ti_3Si_{0.75}Al_{0.25}C_2$, 187 GPa for Ti_3AlC_2 and 197 GPa for Ti_3SiC_2, as illustrated in table 1. The present value for Ti_3SiC_2 is comparable to another *ab initio* calculation (204 GPa) [9]. Although smaller than that of Ti_3SiC_2, the bulk modulus of $Ti_3Si_{0.75}Al_{0.25}C_2$ is very close to that of Ti_3AlC_2. This reveals that high bulk modulus is retained for $Ti_3Si_{0.75}Al_{0.25}C_2$.

3.2. Atomic bonding properties

The fundamental structural element in layered ternary carbides was the edge-shared Ti_6C octahedron. Investigations of the geometry of Ti_6C octahedrons show that the octahedrons distort anisotropically in $Ti_3Si_{0.75}Al_{0.25}C_2$ compared to those in Ti_3SiC_2. The distortions are accommodated by expansion, contraction and rotation of Ti–C bonds in different levels. Two types of deformation for Ti_6C octahedrons are observed. The first one, for which the edge atoms of the octahedron are composed of Ti_I and $Ti_{II,2}$ atoms, is accomplished by $Ti_{I,2}$–C_{II} bond expansion and $Ti_{II,2}$–C_{II} bond contraction. The second type occurs for the octahedron in which edge atoms are composed of Ti_I, $Ti_{II,2}$ and $Ti_{II,1}$. Besides the first distortion mode, it is also accompanied by inclination of the $Ti_{II,2}$ and $Ti_{II,1}$ close-packed plane, which is induced by expansion and rotation of Ti–C bonds.

The properties of covalent bonds could be demonstrated by Mulliken population analysis, which has long been used to indicate the degree of covalency in materials. The method has recently been successfully combined with *ab initio* plane-wave electronic structure calculations [19]. We list the calculated Mulliken populations and bond lengths of covalent bonds in $Ti_3Si_{0.75}Al_{0.25}C_2$ in table 3, together with the corresponding values for Ti_3SiC_2 and Ti_3AlC_2 for comparison. As far as we are aware, no Mulliken population analysis had been

Table 3. Bond lengths and Mulliken populations of covalent bonding in $Ti_3Si_{0.75}Al_{0.25}C_2$, Ti_3SiC_2 and Ti_3AlC_2.

		$Ti_3Si_{0.75}Al_{0.25}C_2$		Ti_3SiC_2		Ti_3AlC_2	
Bond	Component	Population	Bond length	Population	Bond length	Population	Bond length
Ti–C	$Ti_{I,1}$–C_I	0.33	2.1882				
	$Ti_{I,2}$–C_I	0.33	2.1825	0.83	2.1645	0.82	2.1909
	$Ti_{I,2}$–C_{II}	0.32	2.1765				
	$Ti_{II,1}$–C_I	0.52	2.0979				
	$Ti_{II,2}$–C_I	0.52	2.0850	1.43	2.0812	1.52	2.0760
	$Ti_{II,2}$–C_{II}	0.52	2.0749				
Ti–Si	$Ti_{II,1}$–Si	0.38	2.7059	0.76	2.6261		
	$Ti_{II,2}$–Si	0.41	2.6896				
Ti–Al	$Ti_{II,2}$–Al	0.34	2.7165			0.63	2.8592

performed for the Ti_3SiC_2 and Ti_3AlC_2 compounds before. Coinciding with the different levels of internal freedom changes as shown in table 2, the bond lengths yield three values for both Ti_I–C and Ti_{II}–C bonds, and two values for the Ti–Si bond, respectively. In addition, the average bond length of Ti_I–C in $Ti_3Si_{0.75}Al_{0.25}C_2$ increases by 0.83% compared to that in Ti_3SiC_2, and the values increase by 0.23% for the Ti_{II}–C and 2.73% for the Ti–Si bond. With the elongation of average bond lengths, the Mulliken population of covalent bonds is decreased compared to that in Ti_3SiC_2 and Ti_3AlC_2. The population is decreased from 0.84 for Ti_I–C in Ti_3SiC_2 to about 0.33 in $Ti_3Si_{0.75}Al_{0.25}C_2$ and from 1.44 to 0.52 for Ti_{II}–C, respectively. This shows that the degrees of covalency for Ti–C bonds are weakened in $Ti_3Si_{0.75}Al_{0.25}C_2$ from those in Ti_3SiC_2.

Special attention was concentrated on the bonding properties of Ti–Si and Ti–Al atomic bonds. The Mulliken populations yield 0.41 and 0.38 for $Ti_{II,1}$–Si and $Ti_{II,2}$–Si bonds, respectively, which are smaller compared to the corresponding value, 0.76, in Ti_3SiC_2. The difference between $Ti_{II,1}$–Si and $Ti_{II,2}$–Si is attributed to the different coordinating circumstance of Ti with Si or Al atoms. Analogously, the degree of $Ti_{II,2}$–Al covalent bonding is weaker than that in Ti_3AlC_2.

For the layered ternary carbides, the high temperature oxidation resistance was attributed to the weak covalent interactions between the titanium and silicon or aluminium atomic layers. The degrees of covalent bonding of Ti–Si or Ti–Al bonds are weaker than that of Ti–C bonds, which induces the Si or Al atoms to escape outward more easily and form protective oxide scale on the subsurface, such as Al_2O_3 or SiO_2. The properties of covalent bonds in Ti_3SiC_2 and Ti_3AlC_2 are shown in table 3, and the degree of Ti–Al covalent bonding is demonstrated to be weaker than that of the Ti–Si bond. The results suggest that it is easier to form protective Al_2O_3 scale on the subsurface of Ti_3AlC_2. This is supposed to be the intrinsic origin for the better oxidation resistance of Ti_3AlC_2 than Ti_3SiC_2 at high temperature. Applying this hypothesis to the present investigation, we predict that $Ti_3Si_{0.75}Al_{0.25}C_2$ possesses better oxidation resistance than Ti_3SiC_2, because the degrees of Ti–Si and Ti–Al covalent bonding in $Ti_3Si_{0.75}Al_{0.25}C_2$ solid solution are weaker compared to that in Ti_3SiC_2 and Ti_3AlC_2. We are now investigating other important factors that affect the oxidation behaviour of the compounds, such as the minimum energy path of oxygen reacting with atoms on the material surface and outward diffusive energy barriers for Ti, Si and Al atoms.

In order to validate the property prediction on the oxidation resistance, experimental investigations were performed to study the influence of the Al-cementation process on the oxidation behaviour of Ti_3SiC_2-based ceramic [20]. The results showed that Al atoms diffused into the Ti_3SiC_2 specimen easily and partially existed as solid solution atoms. After the cemented Ti_3SiC_2-based ceramic had been oxidized at 1100 °C in air for 20 h, the parabolic rate constant of the specimen was 1.58×10^{-9} kg^2 m^{-4} s^{-1}, decreasing by about two orders of magnitude.

3.3. Electronic band structure analysis

The electronic structures of stoichiometric Ti_3SiC_2 and Ti_3AlC_2 have been clearly revealed before [9, 11]. Some basic features of electronic structure, such as anisotropy, covalency and electrical conductivity, were demonstrated by examining the band dispersion, density of states and distribution of charge density. In this section, we study the characteristics of band structure and density of states of $Ti_3Si_{0.75}Al_{0.25}C_2$, and reveal the effects on electronic band structure after Al substitution.

In figure 2(a), we show the band dispersion curve along some high symmetry directions in the Brillouin zone of $Ti_3Si_{0.75}Al_{0.25}C_2$. Figure 2(b) exhibits the total density of states (TDOS) of the $Ti_3Si_{0.75}Al_{0.25}C_2$ unit cell, together with the TDOS of Ti_3SiC_2 for comparison. It is seen that the valence bands can be divided into several basic groups. The lowest lying group of valence states, which locates at around -12.5 to -9.4 eV, does not change compared to that of Ti_3SiC_2. Between -9.0 and -7.0 eV below the Fermi level, the states are derived from the Si atoms and change distinctly. The states just below the Fermi level are dominated by strongly covalent bonding states of Ti 3d orbitals and C, Si and Al p-derived orbitals. The states near and above the Fermi level contain non-bonding and anti-bonding Ti 3d orbitals.

We have discussed the anisotropic conductivity of Ti_3SiC_2 under various pressures by examining the band dispersion along different high symmetry directions [10]. For $Ti_3Si_{0.75}Al_{0.25}C_2$, less difference of energy dispersion between directions along the *c*-axis and basal plane is observed. This indicates increased isotropy for electrical conductivity after a small number of Si atoms were substituted by Al atoms.

The high electrical conductivity of Ti_3SiC_2 was interpreted in terms of the metallic bond characters near the Fermi level [9, 14]. It still exhibits a typical metallic feature with non-zero density of states at the Fermi level $N(E_F)$ in figure 2(b). As a result, $Ti_3Si_{0.75}Al_{0.25}C_2$ preserves metallic properties, such as metallic conductivity, being analogous to its counterpart, Ti_3SiC_2. In order to roughly estimate the electrical conductivity of $Ti_3Si_{0.75}Al_{0.25}C_2$, we list the $N(E_F)$ values in table 1, together with that of Ti_3SiC_2 and Ti_3AlC_2. This shows that the $N(E_F)$ of $Ti_3Si_{0.75}Al_{0.25}C_2$ is smaller than that of Ti_3SiC_2 but greater than that of Ti_3AlC_2. This indicates that the electrical conductivity of $Ti_3Si_{0.75}Al_{0.25}C_2$ may be located between that of the other two compounds. In order to obtain an insight into the physical nature of the band structure, it is worth examining the projected partial density of states (PDOS) for different types of atom in $Ti_3Si_{0.75}Al_{0.25}C_2$.

Figure 3 shows the PDOS of selected atoms in $Ti_3Si_{0.75}Al_{0.25}C_2$ at the equilibrium geometrical configuration. The PDOS of Ti_I is not illustrated, because it retains similar features to that in Ti_3SiC_2. It is seen in figure 3 that the lowest lying states around -12.5 to -9.4 eV originate predominantly from the C 2s states, which overlap with the Ti 4s and 3d orbitals slightly. The adulteration of Al atoms does not disturb the electronic states in this energy range. The states which locate in the range between -9.0 and -7.0 eV exhibit hybridization of Si 3s–3p and Al 3s–3p orbitals. The characteristics of Al 3s and 3p states resemble those of Si 3s and 3p states in the energy range around -7.5 to -3.0 eV, which indicates that there are

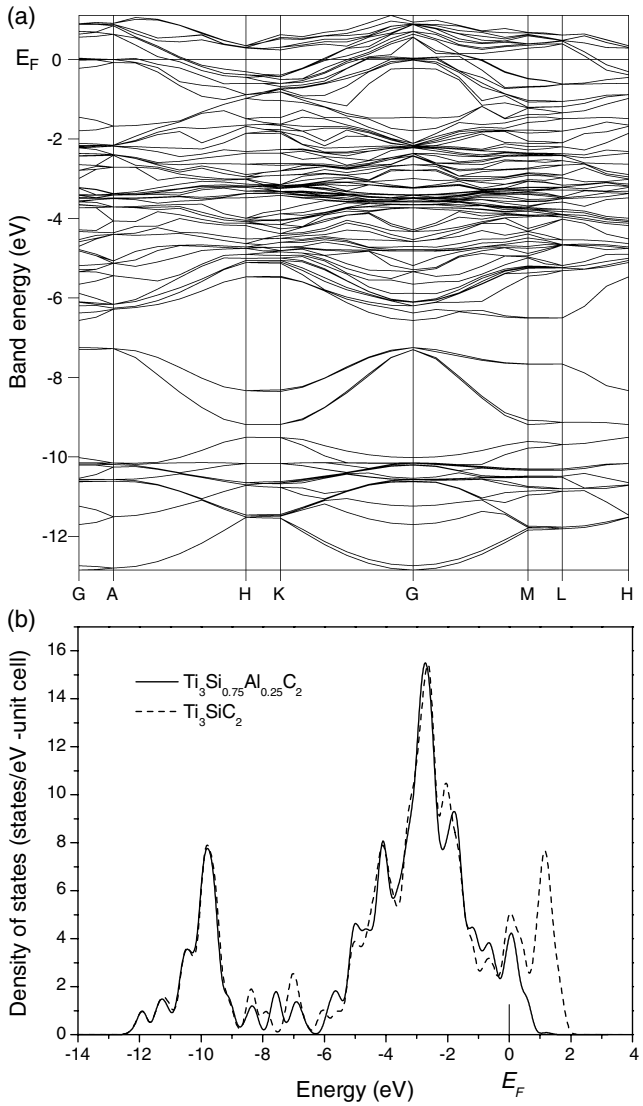

Figure 2. (a) Band dispersion curve of $Ti_3Si_{0.75}Al_{0.25}C_2$ along some high symmetry directions of the BZ and (b) the TDOS of $Ti_3Si_{0.75}Al_{0.25}C_2$ and Ti_3SiC_2.

s–p interactions between Al and Si atoms in the (001)-like close-packed layer. In the energy range from −4.0 to −1.0 eV, there are strongly hybridizing bonded states of Ti 3d orbitals with C, Si and Al p-derived orbitals. For instance, the Ti 3d–C 2p bonding peak locates at around −2.7 eV, the Ti 3d–Si 3p bonding peak at −2.0 eV and the Ti 3d–Al 3p bonding peak at −1.1 eV. We compare the energy values at which the peaks of d–p bonding locate in figure 3 with those in Ti_3SiC_2 and Ti_3AlC_2. It is found that the peak of Ti 3d–Si 3p bonding shifts toward the Fermi level by 0.26 eV, while the hybridization peaks for other d–p bondings are well retained. This means that the degree of Ti–Si covalent bonding is obviously degraded by Al atoms.

Gilman proposed that the chemical bond hardness and mechanical strength or hardness of the covalent compound were determined by the energy gap separating the corresponding

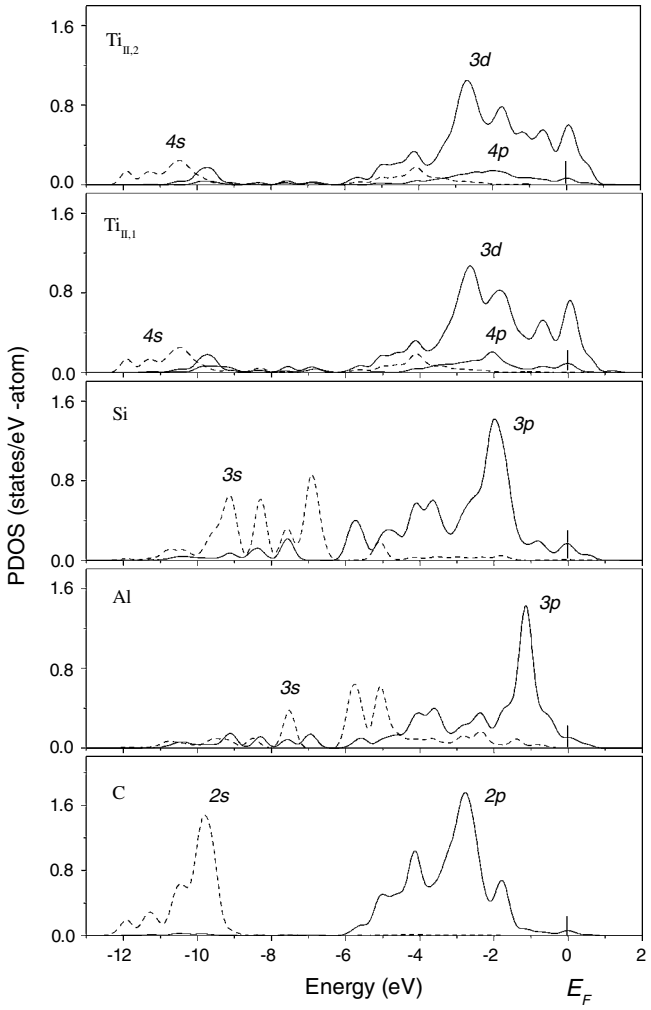

Figure 3. Partial density of states of $Ti_{II,1}$, $Ti_{II,2}$, Si, Al and C atoms in $Ti_3Si_{0.75}Al_{0.25}C_2$.

peaks in the bonding and anti-bonding densities of states [21]. It is noted in figure 3 that the highest occupied bonding peak is attributed to the Al 3p orbital. This induces the corresponding electrons of the Al 3p bonding states to delocalize into the antibonding states more easily when external disturbing conditions are large enough to close the energy gap. In other words, the chemical and mechanical stabilities of $Ti_3Si_{0.75}Al_{0.25}C_2$ are mainly affected by the properties of Al 3p bonding electronic states. It is in the mechanism on the electronic scale that the bulk modulus and oxidation behaviours of $Ti_3Si_{0.75}Al_{0.25}C_2$ resemble that of Ti_3AlC_2. Detailed investigations of the influences of Al atoms on the mechanical properties, such as elastic properties and hardness, are under way, as well as the phase equilibria of $Ti_3(Si_xAl_{1-x})C_2$ solid solution.

4. Conclusion

We have investigated the influences of Al substitution on the equilibrium properties, electronic band structure and atomic bonding for $Ti_3Si_{0.75}Al_{0.25}C_2$ solid solution, by means of first-

principles plane-wave pseudopotential total energy calculations. The lattice constants, atomic internal positions and bond lengths were presented, which were useful in distinguishing the solid solution phase in microstructure observations. We have shown that it is possible for the $Ti_3Si_{0.75}Al_{0.25}C_2$ solid solution phase to co-exist with Ti_3SiC_2 and Ti_3AlC_2 based on comparison of cohesive energies. It has been demonstrated that the degrees of covalency of Ti–Si and Ti–Al bonds in $Ti_3Si_{0.75}Al_{0.25}C_2$ reduced remarkably compared with those in Ti_3SiC_2 and Ti_3AlC_2 compounds, while the isotropy of electrical conductivity increased. The $Ti_3Si_{0.75}Al_{0.25}C_2$ retained excellent bulk modulus like that of Ti_3AlC_2, and possessed optimized oxidation resistance which was verified by isothermal oxidation experiments of Al-cemented Ti_3SiC_2-based ceramic.

Acknowledgments

This work was supported by the National Outstanding Young Scientist Foundation for Y C Zhou under grant No 59925208, the Natural Sciences Foundation of China under grant No 50232040 and the Special Funds for the Major State Basic Research Projects of China (grant No G2000067104), the '863' project, and the High-Tech Bureau of the Chinese Academy of Sciences.

References

[1] Barsoum M W 2000 *Prog. Solid State Chem.* **28** 201
[2] Sun Z M, Zhou Y C and Li M S 2002 *Acta Mater.* **49** 4347
[3] Barsoum M W and El-Raghy T 1997 *J. Electrochem. Soc.* **144** 2508
[4] Wang X H and Zhou Y C 2003 *Corros. Sci.* **45** 891
[5] Nowotny H, Rogl P and Schuster J C 1982 *J. Solid State Chem.* **44** 126
[6] Barsoum M W, Ali M and El-Raghy T 2000 *Metall. Mater. Trans.* A **31** 1857
[7] Barsoum M W, Salama I, El-Raghy T, Golczewski J, Porter W D, Wang H, Seifert H J and Aldinger F 2002 *Metall. Mater. Trans.* A **33** 2775
[8] Medvedeva N I, Novikov D L, Ivanovsky A L, Kuznetsov M V and Freeman A J 1998 *Phys. Rev.* B **58** 16042
[9] Holm B, Ahuja R, Li S and Johansson B 2001 *Appl. Phys. Lett.* **79** 1450
[10] Wang J Y and Zhou Y C 2003 *J. Phys.: Condens. Matter* **15** 1983
[11] Zhou Y C, Wang X H, Sun Z M and Chen S Q 2001 *J. Mater. Chem.* **11** 2335
[12] Gamarnik M Y and Barsoum M W 1999 *J. Mater. Sci.* **34** 169
[13] Pietzka M A and Schuster J C 1997 *J. Phase Equilib.* **15** 392
[14] Zhou Y C, Sun Z M, Wang X H and Chen S Q 2001 *J. Phys.: Condens. Matter* **13** 10001
[15] Payne M C, Teter M P, Allan D C, Arias T A and Joannopoulos J D 1992 *Rev. Mod. Phys.* **64** 1045
[16] Vanderbilt D 1990 *Phys. Rev.* B **41** 7892
[17] Perdew J P and Zunger A 1981 *Phys. Rev.* B **23** 5048
[18] Monkhorst H J and Pack J D 1976 *Phys. Rev.* B **13** 5188
[19] Segall M D, Shah R, Pickard C J and Payne M C 1996 *Phys. Rev.* B **54** 16317
[20] Li M S, Liu G M, Zhang Y M and Zhou Y C 2003 *Oxidation of Metals* **60** 179
[21] Gilman J J 1996 *Mater. Sci. Eng.* A **209** 74